THE JOURNAL OF BIOLOGICAL CHEMISTRY
Vol. 278, No. 49, Issue of December 5, pp. 49191–49195, 2003

Printed in U.S.A.

The Influence of an Intramolecular Hydrogen Bond in Differential Recognition of Inhibitory Acceptor Analogs by Human ABO(H) Blood Group A and B Glycosyltransferases*

Received for publication, August 8, 2003
Published, JBC Papers in Press, September 11, 2003, DOI 10.1074/jbc.M308770200

Hoa P. Nguyen‡, Nina O. L. Seto‡§, Ye Cai¶, Eeva K. Leinala‡, Svetlana N. Borisova‡, Monica M. Palcic¶‖, and Stephen V. Evans‡‡‡**

*From the ‡Department of Biochemistry, Microbiology and Immunology, University of Ottawa, Ottawa, Ontario K1H 8M5, Canada, ¶Department of Chemistry, University of Alberta, Edmonton, Alberta T6G 2V4, Canada, §Institute for Biological Sciences, National Research Council of Canada, Ottawa, Ontario K1A 0R6, Canada, and **Department of Biochemistry and Microbiology, University of Victoria, Victoria, British Columbia V8W 3P6, Canada*

Human ABO(H) blood group glycosyltransferases GTA and GTB catalyze the final monosaccharide addition in the biosynthesis of the human A and B blood group antigens. GTA and GTB utilize a common acceptor, the H antigen disaccharide α-L-Fuc*p*-(1→2)-β-D-Gal*p*-*O*R, but different donors, where GTA transfers GalNAc from UDP-GalNAc and GTB transfers Gal from UDP-Gal. GTA and GTB are two of the most homologous enzymes known to transfer different donors and differ in only 4 amino acid residues, but one in particular (Leu/Met-266) has been shown to dominate the selection between donor sugars. The structures of the A and B glycosyltransferases have been determined to high resolution in complex with two inhibitory acceptor analogs α-L-Fuc*p*-(1→2)-β-D-(3-deoxy)-Gal*p*-*O*R and α-L-Fuc*p*-(1→2)-β-D-(3-amino)-Gal*p*-*O*R, in which the 3-hydroxyl moiety of the Gal ring has been replaced by hydrogen or an amino group, respectively. Remarkably, although the 3-deoxy inhibitor occupies the same conformation and position observed for the native H antigen in GTA and GTB, the 3-amino analog is recognized differently by the two enzymes. The 3-amino substitution introduces a novel intramolecular hydrogen bond between O_2' on Fuc and N3′ on Gal, which alters the minimum-energy conformation of the inhibitor. In the absence of UDP, the 3-amino analog can be accommodated by either GTA or GTB with the L-Fuc residue partially occupying the vacant UDP binding site. However, in the presence of UDP, the analog is forced to abandon the intramolecular hydrogen bond, and the L-Fuc residue is shifted to a less ordered conformation. Further, the residue Leu/Met-266 that was thought important only in distinguishing between donor substrates is observed to interact differently with the 3-amino acceptor analog in GTA and GTB. These observations explain why the 3-deoxy analog acts as a competitive inhibitor of the glycosyltransferase reaction, whereas the 3-amino analog displays complex modes of inhibition.

The human blood group A and B oligosaccharide antigens are respectively formed by the transfer of GalNAc by glycosyltransferase GTA[1] or Gal by glycosyltransferase GTB to the common H-disaccharide α-L-Fuc*p*-(1→2)-β-D-Gal*p*-*O*R, where R is a glycoprotein or glycolipid (1). Generally, humans with the gene for GTA have blood group A, those with GTB have blood group B, those with both genes have blood group AB, and those with neither have blood group O. Glycosyltransferases in general have been implicated as indicators of cancer progression, susceptibility to infectious diseases, glycoprotein activity, and heart and autoimmune diseases (for review, see Ref. 2), and the human ABO(H) blood group glycosyltransferases in particular are viewed as a model system for the study of action and specificity of this class of enzyme.

When the primary structures of GTA and GTB were determined, it was found that they differ in only four amino acid residues which, given that they share a common acceptor, were assumed to confer their ability to distinguish between the donor substrate molecules (3). X-ray crystallographic studies of the catalytic domains of the two enzymes revealed that their structures are almost identical outside of these four residues, that only two of these four residues served to distinguish between donor substrates, and that the acceptor substrate binding sites were nearly superimposable (4).

To assist in further elucidating the mechanisms of these glycosyltransferases, specific analogs of the acceptor molecules were made and characterized kinetically by their ability to inhibit the enzyme reaction. The targeting of the acceptor moiety at the 3-OH linkage site (the point at which the monosaccharide is transferred to the acceptor) of the Gal ring via modification to 3-deoxy and 3-amino analogs (5, 6) produced potent inhibitors of glycosyltransferase activity (Fig. 1). The 3-deoxy analog was found to be a competitive inhibitor of both GTA and GTB, with K_i ranging from 14 to 68 μM, and was shown to inhibit GTA in cell culture such that the expression of surface A antigen was significantly reduced (7). The K_i of the 3-amino analog could not be determined, as the mode of inhi-

* This work was made possible with funding from the Natural Sciences and Engineering Research Council of Canada (to M. M. P.) and Canadian Institutes of Health Research (to S. V. E.). The work at Brookhaven National Laboratories was supported by the U.S. Department of Energy, Division of Materials Sciences and Division of Chemical Sciences, under Contract DE-AC02-98CH10886. The costs of publication of this article were defrayed in part by the payment of page charges. This article must therefore be hereby marked "*advertisement*" in accordance with 18 U.S.C. Section 1734 solely to indicate this fact.

The atomic coordinates and structure factors (codes 1R7T, 1R7U, 1R7V, 1R7X, 1R7Y, 1R80, 1R81, and 1R82) have been deposited in the Protein Data Bank, Research Collaboratory for Structural Bioinformatics, Rutgers University, New Brunswick, NJ (http://www.rcsb.org/).

‖ Member of the Alberta Ingenuity Centre for Carbohydrate Science.

‡‡ To whom correspondence should be addressed: Dept. of Biochemistry and Microbiology, Univ. of Victoria, P.O. Box 3800, STN CSC, Victoria, BC V8W 3P6, Canada. E-mail: svevans@uvic.ca.

[1] The abbreviations used are: GTA, human ABO(H) blood group glycosyltransferase A; GTB, human ABO(H) blood group glycosyltransferase B; CNS, crystallography NMR software; ADA buffer, *N*-[2-acetamido]-2-iminodiacetic acid; Fuc, L-fucose; Gal, D-galactose.

bition for both GTA and GTB was observed not to fit standard models of inhibition. However, it was estimated that K_i for the 3-amino analog is in the 200-nM range for GTA (5, 6).

To understand the different behaviors of the two inhibitors and, specifically, the mode of binding of the 3-amino analog, we determined structures of both GTA and GTB in complex with the 3-deoxy and 3-amino analogs both in the absence and presence of UDP.

MATERIALS AND METHODS

Protein Production—Protein production was carried out as described in Ref. 8.

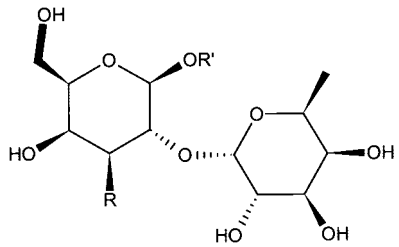

FIG. 1. **Chemical structure of the H-antigen acceptor analogs used to generate complexes with GTA and GTB, where R = H is the 3-deoxy acceptor analog, and R = amino is the 3-amino acceptor analog.** R′ is an aliphatic group used in the purification of the analogs. The native acceptor is given by R = OH.

Inhibitor Synthesis—Acceptor analogs were synthesized as reported previously (5, 6) except for the coupling reaction to produce the protected 3-deoxydisaccharide. For this step, octyl 4,6-O-benzylidene-3-deoxy-β-D-xylo-hexopyranoside (61 mg, 16.7 mmol) and phenyl-2,3,4-tri-O-benzyl-1-thio-β-L-fucopyranoside (105 mg, 20 mmol) were dissolved in dry CH_2Cl_2/ether (6 ml, ratio of 1/5, v/v) at room temperature and cooled to 0 °C. Then *N*-iodosuccinimide (45 mg, 20 mmol) and a catalytic amount of trifluoromethanesulfonic acid were added, and the mixture was stirred for 3 h. The reaction was quenched by the addition of Et_3N. The mixture was diluted with CH_2Cl_2 (20 ml) and washed with saturated Na_2SO_3 (2 × 10 ml), water, and brine. The organic phase was dried over anhydrous Na_2SO_4. Removal of the solvent followed by chromatography on silica gel (6:1, hexane:ethyl acetate) gave the desired 3-deoxydisaccharide as a white solid (96 mg, 74%), which was hydrogenated as originally described.

Protein Crystallization—Crystals of native GTA and GTB were grown as reported previously (4). Crystals were soaked with various combinations of UDP-GalNAc, UDP-Gal, UDP, and acceptor analogs. Soaking solution contained 7.5% polyethylene glycol 4000 (Sigma), 15% glycerol (BDH), 75 mM ADA buffer (Sigma), pH 7.5, 10 mM $MnCl_2$ (Fisher), and 10 mM acceptor for 3–4 days. UDP, UDP-GalNAc, or UDP-Gal (Sigma) was added to the soaking solution at a concentration of 10–15 mM for 20–25 h. At the end of the soaking period, crystals were frozen in liquid propane using magnetic crystal caps (Hampton Research), and the caps were stored in liquid nitrogen for transport to the beamline.

Data Collection and Structure Determination—Data was collected at beamline X8C at the National Synchrotron Light Source at Brookhaven National Laboratories at a wavelength of 1.15 Å. Two data sets

TABLE I
Data collection and structure refinement statistics for GTA and GTB crystallized with inhibitors in the absence of UDP

Data set	GTA + DI[a]	GTB + DI	GTA + AI[b]	GTB + AI
Resolution (Å)	20–2.09	20–1.61	20–2.09	20–1.97
Space group	$C222_1$	$C222_1$	$C222_1$	$C222_1$
a (Å)	52.5	52.6	52.6	52.4
b (Å)	149.5	149.9	150.6	150.2
c (Å)	79.8	79.0	79.7	79.2
R-merge (%)[c,d]	5.1 (37.9)	5.2 (37.0)	4.6 (37.6)	5.6 (38.3)
Completeness (%)[a]	98.1 (96.4)	98.5 (87.4)	96.6 (91.9)	98.3 (99.8)
Unique reflections	18,777	40,504	18,560	22,211
Refinement resolution (Å)	20–2.09	20–1.61	20–2.09	20–1.97
R-work (%)[c,e]	18.8 (20.9)	19.6 (22.1)	19.9 (24.9)	19.3 (19.7)
R-free (%)[c,f]	22.8 (21.4)	20.9 (24.3)	23.7 (27.0)	22.6 (25.9)
rms bond (Å)[g]	0.006	0.005	0.006	0.005
rms angle (°)	1.3	1.3	1.2	1.3

[a] DI = 3-deoxy inhibitor.
[b] AI = 3-amino inhibitor.
[c] Values in parentheses represent highest resolution shell.
[d] *R*-merge, $\Sigma|I_{obs} - I_{ave}|/\Sigma I_{ave}$.
[e] *R*-work, $\Sigma||F_o| - |F_c||/\Sigma|F_o|$.
[f] 10% of reflections were omitted in *R*-free calculations.
[g] rms, root-mean-square.

TABLE II
Data collection and structure refinement statistics for GTA and GTB crystallized with inhibitors in the presence of UDP or UDP-donor

Data set	GTA + AI[a] + UDP	GTB + AI + UDP	GTA + AI + UDP-GalNAc	GTB + AI + UDP-Gal
Resolution (Å)	50–1.75	50–1.65	50–1.75	50–1.55
Space group	$C222_1$	$C222_1$	$C222_1$	$C222_1$
a (Å)	52.5	52.6	52.6	52.8
b (Å)	149.4	150.5	149.4	150.4
c (Å)	79.4	79.3	79.7	79.5
R-merge (%)[b,c]	4.6 (14.8)	3.6 (9.5)	4.0 (14.8)	4.3 (52.5)
Completeness (%)[d]	99.1 (99.0)	99.9 (100)	99.6 (100)	99.1 (97.7)
Unique reflections	32,164	38,315	32,010	45,914
Refinement resolution (Å)	20–1.75	20–1.65	20–1.75	20–1.55
R-work (%)[b,e]	20.7 (19.4)	20.8 (20.4)	21.0 (21.6)	22.2 (25.5)
R-free (%)[b,f]	21.5 (22.4)	22.7 (23.0)	22.3 (23.9)	24.2 (31.6)
rms bond (Å)[g]	0.005	0.005	0.005	0.005
rms angle (°)	1.3	1.3	1.3	1.3

[a] AI = 3-amino inhibitor
[b] Values in parentheses represent highest resolution shell.
[c] *R*-merge, $\Sigma|I_{obs} - I_{ave}|/\Sigma I_{ave}$.
[d] DI, 3-deoxy inhibitor.
[e] *R*-work = $\Sigma||F_o| - |F_c||/\Sigma|F_o|$
[f] 10% of reflections were omitted in *R*-free calculations.
[g] rms, root-mean-square.

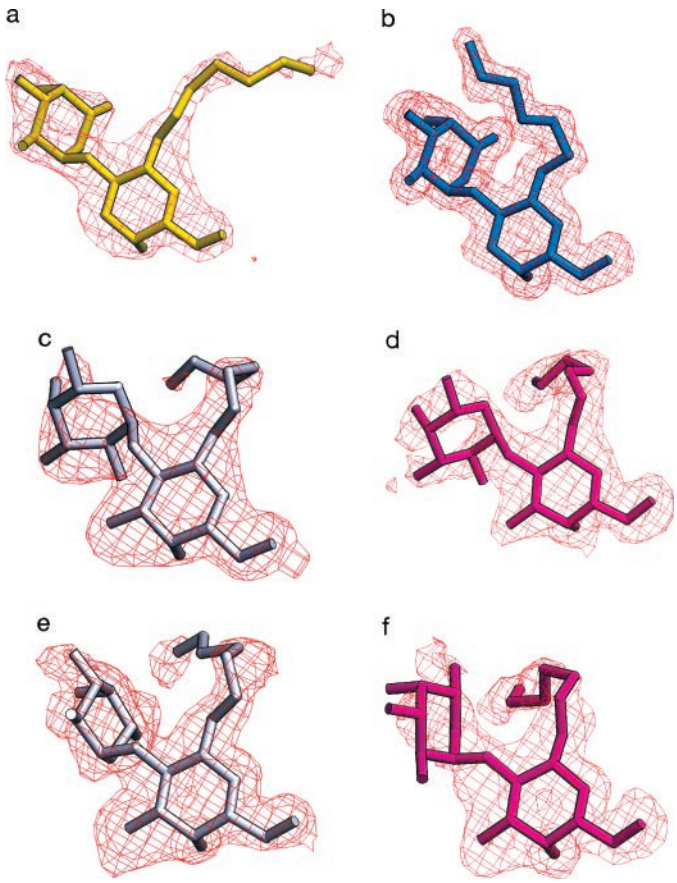

FIG. 2. **Wire-frame models of acceptor analogs co-crystallized with GTA and GTB in the presence and absence of UDP, showing the $2F_o - F_c$ σA electron density in *red* contoured at 0.8 σ.** *a*, DI (*yellow*) bound to GTA in the absence of UDP. *b*, DI (*blue*) bound to GTB in the absence of UDP. *c*, AI (*white*) bound to GTA in the absence of UDP. *d*, AI (*magenta*) bound to GTB in the absence of UDP. *e*, AI (*white*) bound to GTA in the presence of UDP. *f*, AI (*magenta*) bound to GTB in the presence of UDP.

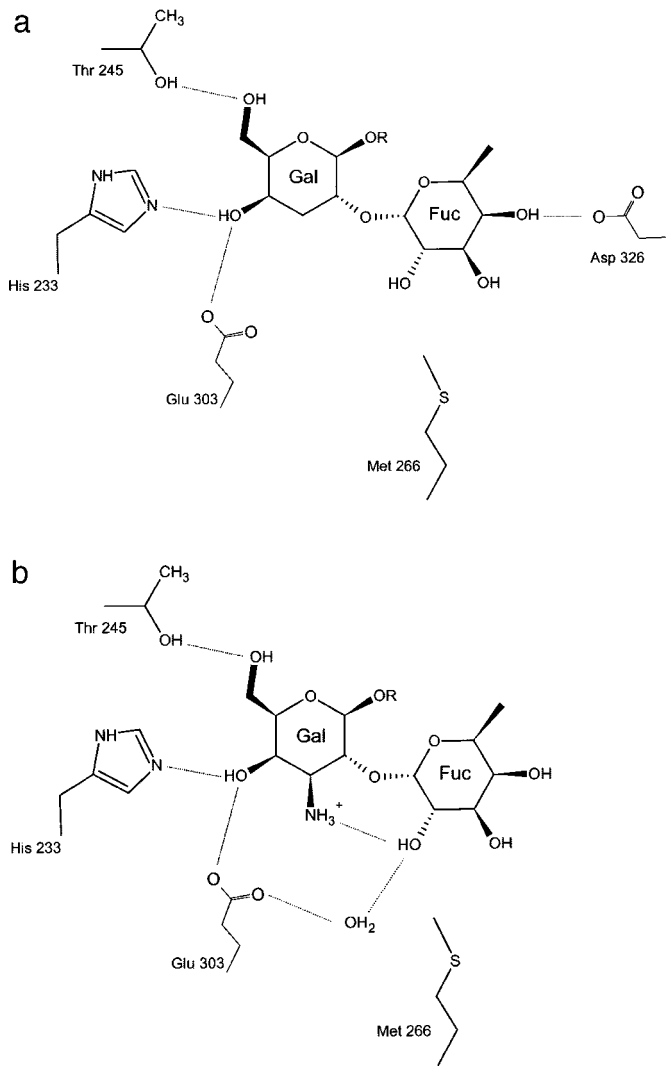

FIG. 3. **Significant contacts observed between GTB and 3-deoxy inhibitor (*a*) and 3-amino inhibitor (*b*), both in the absence of UDP.** The contacts made by GTA with these two acceptor analogs are similar except for Leu-266, which makes no contact with the 3-amino analog.

(GTA+DI and GTA+AI) were collected on a MAR 300 mounted on a Rigaku RU300 generator at Queen's University (Kingston, Ontario, Canada). All data were collected at low temperature using a Cryostream 600 cooler. Data was reduced and scaled with HKL2000 software (9). Initial rigid body refinement in CNS (10) was carried out by using the native GTA and GTB structures with and without H-antigen and UDP bound (PDB codes 1LZ0, 1LZ7, 1LZI, and 1LZJ). This procedure was followed by overall structural refinement using CNS. Least-squared overlaps of structures were calculated by using LSQKAB within the CCP4 program suite (11). All overlaps shown are based on protein-protein overlaps to the GTB structure (PDB code 1LZJ). Diagrams were made using ChemSketch and SETOR (12).

RESULTS

Data Collection and Structure Refinement—Details of the data collection and structure refinement are shown in Tables I and II. Data were collected to a maximum of 2.09–1.55 Å resolution, with R and R_{free} for the final models from ~0.188–0.208 and from 0.209–0.227, respectively. All structures show excellent electron density over the course of the polypeptide chain, with the exception of the disordered loop between residues 177–195 and the final 10 residues of the C terminus, which were also absent in the native structures (4). These data sets (see Table I) are GTA + 3-deoxy inhibitor (GTA+DI), GTB + 3-deoxy inhibitor (GTB+DI), GTA + 3-amino inhibitor (GTA+AI), and GTB + 3-amino inhibitor (GTB+AI). UDP was present in the soaking solution of four crystals, and UDP appears clearly in the corresponding electron density maps. These data sets (see Table II) are GTA + 3-amino inhibitor + UDP (GTA+AI+UDP), and GTB + 3-amino inhibitor + UDP (GTB+AI+UDP). GTA and GTB were also co-crystallized with 3-amino inhibitors in the presence of UDP-GalNAc and UDP-Gal, respectively, (GTA+AI+UDP-GalNAc and GTB+AI+UDP-Gal). The structures have been deposited with the Protein Data Bank with accession codes 1R7T, 1R7U, 1R7V, 1R7X, 1R7Y, 1R80, 1R81, and 1R82, respectively.

DISCUSSION

Structural Analysis of 3-Deoxy Acceptor Analog—The 3-deoxy acceptor analog of the H-disaccharide bound to both GTA and GTB in the absence of UDP (Fig. 2, *a* and *b*), which was surprising given that UDP is known to form an integral part of the acceptor-binding site (4). This 3-deoxy inhibitor has the same overall conformation and binding interactions observed for the GTA and GTB structures containing H-antigen and UDP (Fig. 3*a*; Ref. 4). No significant changes in polypeptide structures were observed. The acceptor analog displayed the same position and orientation in the binding site as the native acceptor (Fig. 4*a*; Ref. 4). As in the structures of the native enzymes, the aliphatic tail of the acceptor analog occupies a different specific location in GTA and GTB due to the presence of Ser-235 in GTB compared with the Gly-235 in GTA (Fig. 2, *a*

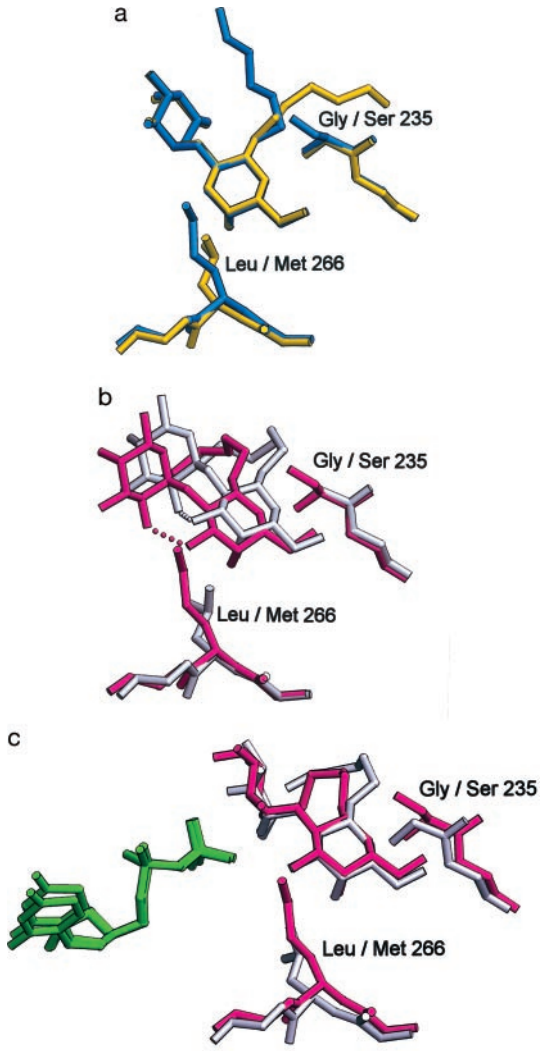

FIG. 4. **Superposition of the binding pockets of GTA and GTB with the acceptor analogs, showing the relative positions of critical residues Leu-266 and Gly-235 (GTA) and Met-266 and Ser-235 (GTB).** *a*, DI bound to GTA (*yellow*) and GTB (*blue*). *b*, AI bound to GTA (*white*) and GTB (*magenta*) in the absence of UDP. *c*, AI bound to GTA (*white*) and GTB (*magenta*) in the presence of UDP (*green*).

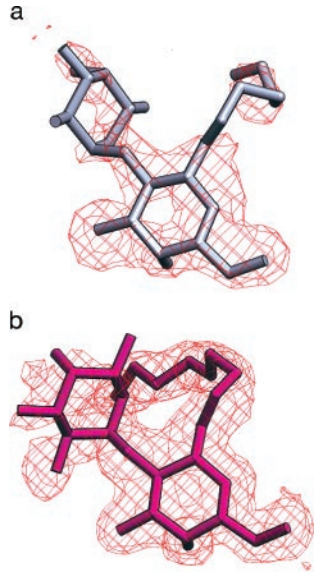

FIG. 5. **Wire-frame models of acceptor analogs co-crystallized with GTA (*white*) and GTB (*magenta*) in the presence and absence of UDP-donor sugars, showing the $2F_o - F_c$ σA electron density in *red* contoured at 0.8 σ.** *a*, AI bound to GTA crystallized in the presence of UDP-GalNAc. *b*, AI bound to GTB crystallized in the presence of UDP-Gal.

and *b*; Ref. 4). The conformation and orientation of the deoxy analog did not change with the presence of UDP (structures not shown). These observations are consistent with the kinetic results reported for the 3-deoxy analog that characterize it as a competitive inhibitor of the H-antigen with well defined behavior (5).

This analog differs from the H-disaccharide acceptor by the lack of the 3-OH group on the Gal residue and so prevents the transfer of saccharide from donor; it was hoped that this difference would allow the co-crystallization of enzyme with acceptor analog and donor. However, experiments to co-crystallize UDP-GalNAc and UDP-Gal with GTA and GTB, respectively, did not yield any electron density corresponding to the donor sugar. (Electron density consistent with partial occupancy by UDP was observed similar to that described for the 3-amino inhibitor, below.)

Structures of 3-Amino Acceptor Analog—Unlike the 3-deoxy inhibitor, the kinetic data regarding the 3-amino analog indicated that there was a complex mode of binding involved in its inhibition of both GTA and GTB (6). Fig. 2 shows the electron density surrounding the acceptor analogs in GTA and GTB complexed to the 3-amino analog crystallized in the absence (Fig. 2, *c* and *d*) and presence (Fig. 2, *e* and *f*) of UDP. In the absence of UDP, the analog is seen to adopt a conformation that is significantly different from that observed for either the native acceptor or 3-deoxy analog, which is induced by the presence of the amino group. This group would be protonated at physiological pH and is observed in the crystal structures of the complexes to form a hydrogen bond with hydroxyl on O-2′ of the fucose residue. This new conformation has the Gal residue in approximately the same location as the native acceptor, with the maintenance of the O-4′ and O-6′ hydrogen bonds observed in other structures (Fig. 3*b*), with the result that the L-Fuc residue moves sharply toward the surface of the protein pocket and into the space normally occupied by UDP. This new position is further stabilized by the formation of a new hydrogen bond from Fuc O-2′ through a bridging water molecule to potential nucleophilic residue Glu-303 in both GTA and GTB (Figs. 3*b* and 4*b*).

In the presence of UDP, the Gal moiety of the 3-amino analog remains in approximately the same position observed for the native acceptor and deoxy analog. The fucose residue is thus displaced, causing the 3-amino analog to abandon the intramolecular hydrogen bond and the hydrogen bond to the bridging water molecule. The fucose ring takes up a less ordered position, with no apparent contact with any part of the enzyme (Fig. 4*c*), and displays significantly higher temperature factors than the Gal residue.

As with the 3-deoxy analog, attempts made to co-crystallize the 3-amino analog with GTA and GTB in the presence of UDP-GalNAc and UDP-Gal did not reveal a density corresponding to either donor; however, as was found for the deoxy analog, the enzyme was able to hydrolyze significant amounts of donor over the crystallization experiments such that partial occupancy for UDP was observed. In these crystal structures (GTA+AI+UDP-GalNAc and GTB+AI+UDP-Gal), excellent density was observed for the Gal residue, but the L-Fuc residue was disordered, especially in GTA (possibly over the two basic conformations observed), to the extent that the electron density corresponding to this residue was poorly defined (Fig. 5, *a* and *b*).

The repositioning of the 3-amino acceptor analog is not restricted to the influence of UDP alone, and Fig. 4*b* shows that, in the absence of UDP, the analog occupies distinctly different positions in GTA and GTB, which correspond to changes in the identity of amino acid residue 266. Of the four amino acid differences between GTA and GTB, residue 266 has been shown to dominate the selection between UDP sugar donors (4), with GTA having Leu and GTB having Met. Small differences between the binding of H-disaccharide acceptor to GTA and GTB have been noted in the past (8) and attributed to Leu/Met-266; however, the positions of both the native (4) and now the 3-deoxy acceptor analogs in GTA and GTB are nearly superimposable. The large difference in position observed for the 3-amino analog emphasizes the influence that Leu/Met-266 can have on acceptor binding.

Finally, although the aliphatic aglycones are placed to aid in the purification of the acceptor analogs, they are attached at the same position as the natural glycoprotein or glycolipid substrate of the A and B antigens, and their conformations give some insight into the differential recognition of these substrates by GTA and GTB (4). Fig. 4*a* shows the positions of the aliphatic groups observed for the deoxy acceptors, where the difference in conformation is similar to that observed in the native acceptors and can be attributed to one of the four critical residue differences between GTA and GTB (Gly/Ser-235). The observed movement of the Fuc residue to form a hydrogen bond with the 3-amino Gal in the absence of UDP opens a pocket in the binding site into which the aliphatic tail moves (Fig. 4*b*). The presence of UDP in the binding site causes the Fuc ring on the inhibitor to become disordered but still permits the aliphatic aglycone to assume the same general conformation.

CONCLUSIONS

The x-ray crystal structures of the 3-deoxy and 3-amino analogs in complex with GTA and GTB show that the binding of these modified H-antigen acceptor analogs are consistent with their observed activity as inhibitors of acceptor binding in GTA and GTB. The binding of the 3-amino analog takes a marked departure from that displayed by the H-disaccharide acceptor and 3-deoxy analog, where this binding changes in the presence or absence of UDP. Remarkably given that GTA and GTB share a common acceptor, the binding of acceptor analog is significantly affected by whether the enzyme is GTA or GTB. The competition of the 3-amino acceptor with UDP for the same binding site in the protein is consistent with the observed complex mode of inhibition.

Acknowledgments—We thank Professor Ole Hindsgaul for providing both guidance and the facilities for the re-synthesis of the 3-amino inhibitor. We thank Rob Polakowski and Ho Jun Lee for aid in the purification of protein, as well as the National Synchrotron Light Source staff at beam lines X8C and X12C at Brookhaven National Laboratories in Long Island, New York.

REFERENCES

1. Watkins, W. M. (1980) in *Advances in Human Genetics* (Harris, H., and Hirschhorn, K., eds) Vol. 10, pp. 1–136, Plenum Publishing Corp., New York
2. Greenwell, P. (1997) *Glycoconj J.* **14,** 159–173
3. Yamamoto, F., Clausen, H., White, T., Marken, J., and Hakomori, S. (1990) *Nature* **345,** 229–233
4. Patenaude, S. I., Seto, N. O., Borisova, S. N., Szpacenko, A., Marcus, S. L., Palcic, M. M., and Evans, S. V. (2002) *Nat. Struct. Biol.* **9,** 685–690
5. Lowary, T. L., and Hindsgaul, O. (1993) *Carbohydr. Res.* **249,** 163–195
6. Lowary, T. L., and Hindsgaul, O. (1994) *Carbohydr. Res.* **251,** 33–67
7. Laferte, S., Chan, N. W., Sujino, K., Lowary, T. L., and Palcic, M. M. (2000) *Eur. J. Biochem.* **267,** 4840–4849
8. Marcus, S. L., Polakowski, R., Seto, N. O., Leinala, E., Borisova, S., Blancher, A., Roubinet, F., Evans, S. V., and Palcic, M. M. (2003) *J. Biol. Chem.* **278,** 12403–12405
9. Otwinowski, Z., and Minor, W. (1997) *Methods Enzymol.* **276,** 307–326
10. Brunger, A. T., Adams, P. D., Clore, G. M., DeLano, W. L., Gros, P., Grosse-Kunstleve, R. W., Jiang, J. S., Kuszewski, J., Nilges, M., Pannu, N. S., Read, R. J., Rice, L. M., Simonson, T., and Warren, G. L. (1998) *Acta Crystallogr. Sec. D.* **54,** Pt. 5, 905–921
11. Collaborative Computational Project Number 4 (1994) *Acta Crystallogr. Sec. D.* **50,** 760–763
12. Evans, S. V. (1993) *J. Mol. Graphics* **11,** 127–138